ADVANCED FUNCTIONAL MATERIALS
www.afm-journal.de

A New Paradigm for Materials Discovery: Heuristics-Assisted Combinatorial Chemistry Involving Parameterization of Material Novelty

*Woon Bae Park, Namsoo Shin, Kun-Pyo Hong, Myoungho Pyo, and Kee-Sun Sohn**

The combinatorial chemistry (combi-chem) of inorganic functional materials has not yet led to the discovery of commercially interesting materials, in contrast to the many successful discoveries of heterogeneous catalysts leading to commercialization. Novel materials for practical use are likely hidden in the multicompositional search space that contains an infinite number of possible stoichiometries, as well as a large number of well-known materials. To discover new, inorganic luminescent materials (phosphors) from the SrO-CaO-BaO-La_2O_3-Y_2O_3-Si_3N_4-Eu_2O_3 search space, heuristics optimization strategies, such as the non-dominated-sorting genetic algorithm (NSGA) and particle swarm optimization (PSO) are coupled with high-throughput experimentation (HTE) in such a manner that the experimental evaluation of fitness functions for the NSGA and PSO is accomplished by the HTE. The proposed strategy also involves the parameterization of the material novelty to avoid systematically a futile convergence on well-known, already-established materials. Although the process starts with random compositions, we finally converge on a novel, single-phase, yellow-green-emitting luminescent material, $La_{4-x}Ca_xSi_{12}O_{3+x}N_{18-x}:Eu^{2+}$, that has strong potential for practical use in white light-emitting diodes (WLEDs).

1. Introduction

Since the first combinatorial chemistry (combi-chem) of inorganic luminescent materials (phosphors),[1–6] it has been employed in an attempt to discover novel phosphors for use in various applications.[7–14] Meanwhile, the demand for new phosphors has been rising sharply because phosphors have become a key material in white light-emitting diodes (WLEDs), which have attracted a great deal of attention for their advantages in terms of energy saving and environmental friendliness.[15] Despite the successful development of high-throughput experimentation (HTE) based on thin-film or inkjet techniques, it has never led to any noteworthy phosphors for use in practical applications, including WLEDs.

Although we evaluated the combi-chem-assisted discovery of a new phosphor, Sr_2CeO_4, to be highly valuable in terms of scientific merit,[2] its practicality was limited. The related industries did not seem to be interested in it, so it was never used in any actual applications. The phosphors discovered in other previous combi-chem work, even including our reports,[8–11] have also been, unfortunately, less than pragmatic. Consequently, the phosphors discovered through the previous combi-chem approaches had valuable scientific merit, but did not interest the related industries. This situation contrasts with the brilliant discovery of new, commercially available WLED phosphors during the same period, using conventional one-by-one methods based on intuition and knowledge.[16–19] This means that, as far as phosphor discovery was concerned, combi-chem was defeated by the conventional trial-and-error method. That's why combi-chem has been criticized as only a methodology for methodology's sake. It is our opinion that combi-chem should lead to the substantial development of engineering materials that are ready for use in industry.

The conventional combi-chem of inorganic functional materials has focused mostly on the development of smart, efficient HTE systems and only, to a limited extent, on data mining and virtual screening.[20–25] Even when a well-established HTE system is secured, however, it is impossible to track down the nearly infinite number of possible combinatorial candidates in the huge, multicompositional search space that transcends conventional ternary or quaternary libraries. Thus, the experimental planning (or design) should be done carefully to reduce the cost and energy consumption of the combi-chem. It is also very important to avoid the futile discovery of well-known materials that exist in the multicompositional search space of interest. For instance, if combi-chem were designed only to pursue a high-luminescence efficacy, then it would definitely end up with one of many well-known phosphors that already reside in the search space. Therefore, a criterion by which we can judge the novelty of the materials should be taken into account, and special measures should

W. B. Park, Prof. M. Pyo, Prof. K.-S. Sohn
Department of Printed Electronics Engineering
World Class University (WCU) Program
Sunchon National University
Maygok dong 315, Sunchon, Chonnam 540-742, Korea
E-mail: kssohn@sunchon.ac.kr
Dr. N. Shin
Pohang Accelerator Laboratory
Pohang University of Science and Technology
Pohang, Kyungbuk 790-784, Korea
Dr. K.-P. Hong
Neutron Science Division
Korea Atomic Energy Research Institute
Daejeon 305-353, Korea

DOI: 10.1002/adfm.201102118

be taken to avoid the futile recurrence of well-known materials and thereby to guarantee a novel discovery.

To sort out the combi-chem issues, we employed heuristics optimization involving a parameterization of the material novelty. We used a non-dominated-sorting genetic algorithm (NSGA)[26,27] for a preliminary screening of the multidimensional search space, and particle swarm optimization (PSO)[28] for the ensuing fine-tuning in a reduced composition space to narrow the possibility of discovery. We also created a parameter designating the novelty of the phosphors, the so-called structural rank, and used it as an objective (fitness) function in the NSGA.

2. Distinction of the Suggested Materials Discovery Strategy

Except for the use of the genetic algorithm (GA) for either virtual screening or data mining,[20–25] there have been only a few cases in which heuristics optimization has been coupled with HTE.[10–12,29,30] When coupled with HTE, GA has been versatile for the discovery of heterogeneous catalysts,[31–33] membranes[29] and phosphors.[10–12] In contrast to the previous cases, however, in which only a simple GA was used, the present study deals with the systematic combination of NSGA and PSO along with the parameterization of the material novelty (the structural rank) to discover novel (oxy)nitride phosphors for use in WLEDs. Although GA has been used previously for the combi-chem of inorganic materials, PSO and the structural rank have never been used before.

What distinguishes the suggested discovery strategy from conventional methods is summarized schematically in **Figure 1**, wherein the current status of combinatorial materials science is well described. The schematic diagram in Figure 1 shows four different combi-chem routes for inorganic materials discovery, marked by the numbers in red. Route 4 is our concern in the present study. The other routes are well-known, but they do not seem to be promising in terms of the chances for the successful discovery of new materials. The two question marks indicate the skepticism about routes 1, 2 and 3. Because routes 1 and 2 also utilize heuristics optimization such as GA, one might be confused between these previous cases and our approach. However, the distinction is made clear by the fact that the use of heuristics in our case includes experimental fitness evaluation for the direct discovery of new materials, while the other cases all deal with an equation-type model as a fitness function. The final outcome in the cases of routes 1 and 2 is not an actual discovery, but just a prediction. The prediction does not guarantee a 100% successful discovery of a new material. Route 3 seems ineffective because it depends only on the arbitrary choice of the search space with, at best, ternary and quaternary compositional systems. The distinctive key ideas of the present approach are the combination of NSGA and PSO with the parameterization of the material novelty, and, more importantly, the HTE-based experimental fitness evaluation for the NSGA and PSO should be noted.

The main problem in cases in which a heuristics optimization strategy such as GA has been used in combi-chem is the fitness function. Since experimental fitness evaluation is sluggish, expensive and sometimes even impossible, the search goes on for computational methods research) that reliably predict the properties of a material (route 1 in Figure 1). In the absence of such methods, data-mining simulators, such as simple, linear (or non-linear) models, support-vector machines, artificial neural networks, B-splines and kriging, can be employed to model the limited amount of data obtained either from HTE or from databases, so that the simulator can be regarded as a fitness function for GA (route 2 in Figure 1). In contrast to cases in which such equation-type fitness functions are available, however, an equation-type fitness function did not exist in the present study. Only the experimental evaluation of the fitness function was available by characterizing actually synthesized phosphor samples. Specifically, we synthesized a number of phosphors using a solid-state powder synthesis-based HTE, and measured photoluminescence (PL) and X-ray-diffraction (XRD) data in a pseudo-HTE manner. Thereafter, the PL intensity and the novelty of structure (the structural rank) were assigned to each phosphor sample and used as fitness functions in the NSGA. Of course, the subsequent PSO process also adopted the HTE-based experimental fitness evaluation.

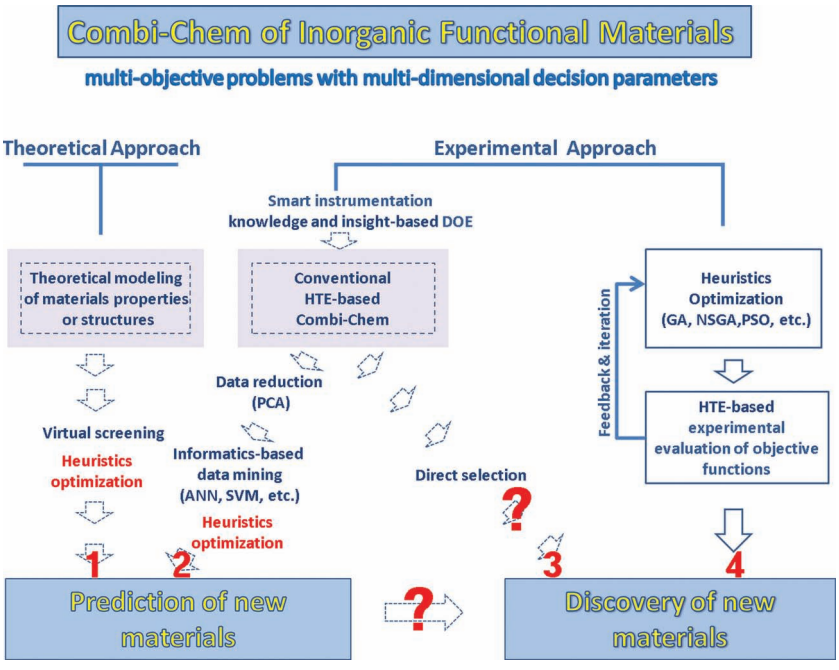

Figure 1. The current status of the combi-chem of inorganic functional materials.

The suggested discovery strategy consists of 3 sequential steps, as summarized schematically in **Figure 2.** The first step is to design a decision parameter (composition) space, based on knowledge, insight and the current industry demand. The second step is to pinpoint a novel phosphor by implementing an NSGA- and PSO-assisted combinatorial materials search (NSGACMS and PSOCMS), complemented by the parameterization of the material novelty. The last step is to

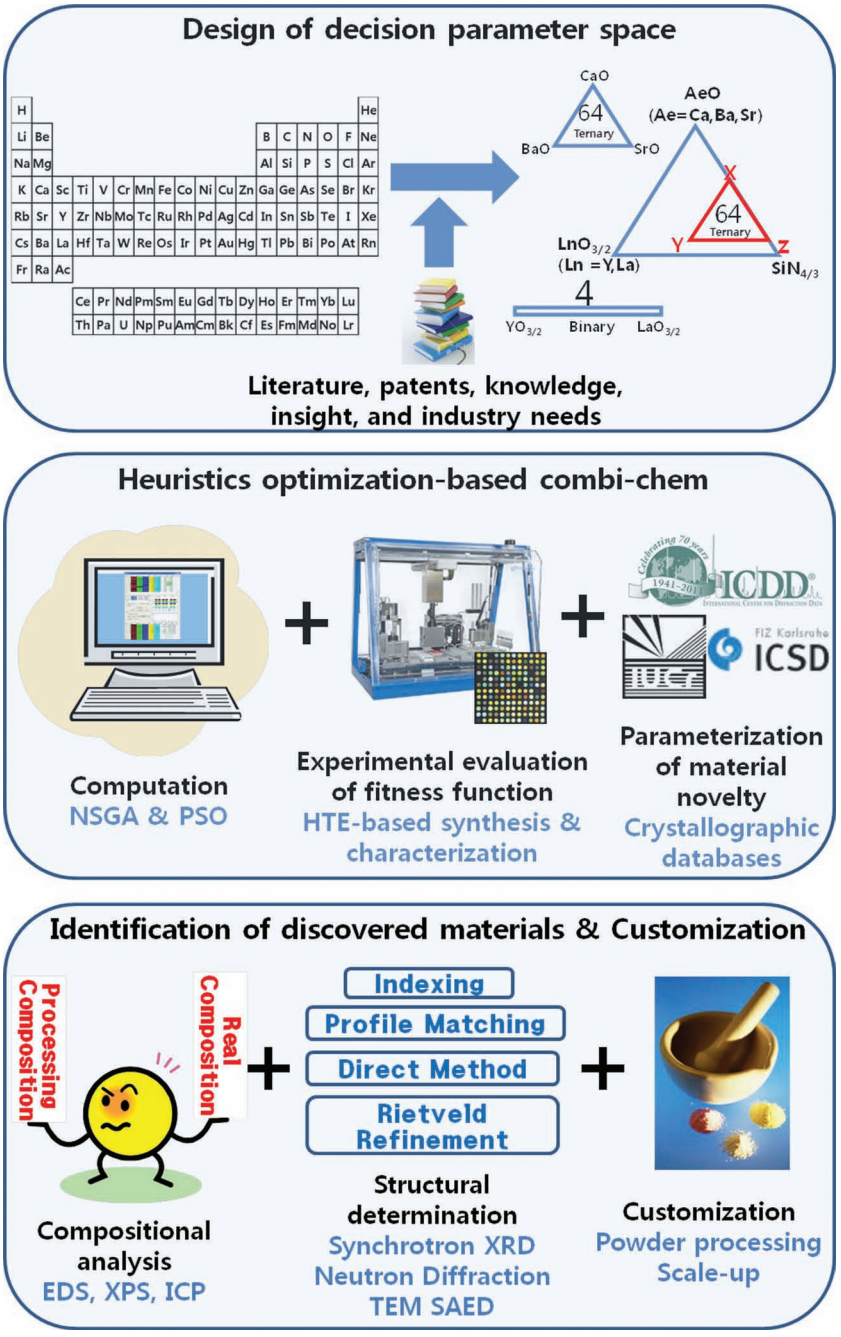

Figure 2. Overall description of the proposed discovery process for new luminescent materials.

identify the discovered material based on conventional compositional and structural analyses. The last step also involves a customization process.

3. NSGACMS and PSOCMS for Discovery of Novel Phosphors

The recent trend in WLED phosphors has changed from traditional oxide-, (oxy)sulfide- and (oxy)halide-based hosts to (oxy)nitride-based hosts, due to their superiority in terms of luminescent efficacy, color rendering, thermal stability, etc.[16–19] The possibility of discovering new phosphors in the (oxy)nitride composition space appears higher, whereas the oxide-, (oxy)sulfide- and (oxy)halide-based compositions have been already exploited. We adopted the SrO-CaO-BaO-La_2O_3-Y_2O_3-Si_3N_4-Eu_2O_3 search space based on the current trend in WLED phosphors, (i.e., by referring to the literature, patents and industry demand). One might wonder why we did not adopt a larger composition search space to achieve a complete optimization in one effort. As an extreme example, one might think of the entire periodic table as a search space. If such a huge search space were adopted, then it would require a larger population size and a higher number of iterations, including a huge number of unnecessary samples. Since our fitness evaluation process was implemented by the actual HTE-based synthesis and characterization of phosphors, it would be impossible and unnecessary to incorporate such a huge search space, although a promising HTE system was employed. The larger the search space, the larger the experimental burden. In this regard, we ruled out unnecessary elements and incorporated only several plausible elements, the choice of which was based on pre-knowledge acquired from the literature, patents and, more importantly, the current industry trends. Accordingly, we adopted the reasonably reduced search space of SrO-CaO-BaO-La_2O_3-Y_2O_3-Si_3N_4-Eu_2O_3 (Figure S2, Supporting Information). The composition of many well-known (oxy)nitride phosphors was primarily taken into account in the choice of this search space, (i.e., the search space was designed to exclude many well-known phosphors). In spite of such an effort, the chosen composition space in which NSGA and PSO were implemented still included many well-known phosphors.

The chosen composition space was full of luminescent materials, even including well-known ones. Therefore, it should be noted that our goal was not to simply discriminate luminescent materials from a lot of non-luminescent materials in the impractical search space, but to pinpoint a novel, brilliant one among all of those that gave acceptable luminescence. If NSGA and PSO had not been used, it would have been necessary to synthesize and characterize 16 384 phosphor samples for full screening of the search space (Figure S2, Supporting Information). Because it is practically impossible to perform such a huge task using solid-sate powder synthesis-based HTE, the use of NSGA and PSO should inevitably relieve the experimental burden and prevent the futile discovery of well-known phosphors.

The PL intensity and structural rank were adopted as fitness functions in NSGACMS and PSOCMS, and only the phosphor composition was dealt with as a decision parameter. As for the choice of fitness functions and decision parameters in the NSGACMS and PSOCMS implementation, one may question why we did not consider the spectral distribution of PL as a fitness function and as to why we did not incorporate processing parameters, such as firing temperature, gas flow, firing time, sintering additives, etc., as decision parameters.

Besides the PL intensity, the spectral distribution is also important because it is closely related to color temperature, color rendering, color chromaticity, etc. The spectral distribution of emissions, namely, the emission color, was not taken into account in the NSGACMS and PSOCMS. Only the PL intensity was used as a fitness function, along with the structural rank. This is sensible if we consider the fact that the aim of our NSGACMS was not the discovery of a phosphor by targeting a predetermined, particular PL property, but the discovery of phosphors with new structures that will not cause any conflicts with the intellectual property of existing phosphors. It is obvious that color control can be achieved to a certain extent by fine-tuning the composition once the structure is well-established.

In principle, it might be more promising to incorporate all of the processing parameters as decision parameters in the NSGA and PSO. However, we concluded that it was more economical to fix the processing conditions than to incorporate processing parameters. Besides the economic reasoning, however, preliminary experiments gave us a reasonable rationale for the use of a fixed processing condition. We performed preliminary experiments; that is, we synthesized the first generation of NSGACMS several times under different processing conditions, in order to fix the best processing conditions in the composition search space of concern. A change in processing conditions made no big difference to the PL and structure of most of the samples in the first generation because we had already reduced the search space in advance. It should be noted that our goal was not simply to discriminate luminescent materials from a lot of non-luminescent materials in the impractical search space, but to pinpoint a novel, brilliant one in a carefully reduced search space. Almost all of the samples in the reduced space gave acceptable luminescence in our fixed processing condition. Consequently, the fixed processing condition was reasonable.

Prior to the discovery of new phosphors, we had to clarify what is meant by that term. The classification presented in **Table 1** was reasonably determined based on the history of recently developed, commercially available WLED phosphors. These criteria can be applied not only to phosphors, but also to any other inorganic functional materials. Only Type III and Type IV, which have yet to be patented, should be considered significant discoveries. Therefore, we had to pursue the discovery of Type-III and Type-IV phosphors to avoid intellectual property complications. Combi-chem has not previously led to the discovery and commercialization of either Type-III or Type-IV phosphors. Only the futile recurrence of well-known phosphors or, at best, Type-II phosphors has been possible.[1–14] A simple trial-and-error approach with minimal insight into materials science should be sufficient for the discovery of Type II, without the high-cost combi-chem approach. Accordingly, the discovery strategy was tailored to target only Type III and Type IV.

Table 1. The categorization of new phosphors for use in WLEDs.

Type of New WLED phosphors	Definition	Example Chemical Formula (conventional title)
Type I	Discovered long ago, but has recently been used in new applications	$Y_3Al_5O_{12}:Ce^{3+}$ (YAG) $Sr_2SiO_4:Eu^{2+}$ (Orthosilicate)
Type II	Slightly altered composition, but the same structure as well-known phosphors – partially substituted solid - solution type	(Tb or Lu)$_3$(Al,Ga)$_5O_{12}:Ce^{3+}$ (TAG or LUAG) (Sr, Ba, Mg)$_2SiO_4:Eu^{2+}$ (Sr, Ca)$AlSiN_3:Eu^{2+}$ (SCASIN)
Type III	Well-known host structure, but has never been considered as a phosphor	α-, β-SIALON $CaAlSiN_3:Eu^{2+}$ (CASIN)
Type IV	New phosphor with the host structure unknown – the correct structural determination should be involved in the discovery process	$Ba_3Si_6O_{12}N_2:Eu^{2+}$ (BSON)

Table 2. Detailed descriptions of the structural ranks.

	Description
1st rank	Unknown phase with negligible minor phases.
2nd rank	Unknown phase as the major constituent and known phase (which has never served as a phosphor) as a minor constituent.
3rd rank	Unknown phase as the major constituent and starting materials or well-known phosphor as a minor constituent.
4th rank	Known phase (which has never served as a phosphor) as the major constituent and unknown phase as a minor constituent.
5th rank	Known phase (which has never served as a phosphor) with negligible minor phases.
6th rank	Known phase (which has never served as a phosphor) as the major constituent and starting materials as a minor constituent.
7th rank	Known phase (which has never served as a phosphor) as the major constituent and well-known phosphor as a minor constituent.
8th rank	Starting materials as the major constituent and unknown phase as a minor constituent.
9th rank	Starting materials as the major constituent and known phase (which has never served as a phosphor) as a minor constituent.
10th rank	Starting materials with negligible minor phases
11th rank	Starting materials as the major constituent and well-known phosphor as a minor constituent.
12th rank	Well-known phosphor as the major constituent and unknown phase as a minor constituent.
13th rank	Well-known phosphor as the major constituent and known phase (which has never served as a phosphor) as a minor constituent.
14th rank	Well-known phosphor as the major constituent and starting materials as a minor constituent.
15th rank	Well-known phosphor with negligible minor phases.
16th rank	Powder form with a certain XRD pattern but no luminescence.
17th rank	Melted, blackened, tarnished, volatilized, etc.

To converge on new Type-III and Type-IV phosphors, we took special measures to make the NSGACMS process stick to these materials. The structural rank, which represents the novelty of the host structure, was used as a fitness function to be minimized in the NSGACMS process, while the PL intensity was adopted as the other fitness function, to be maximized simultaneously. It is impossible to perform conventional structural analysis in the sequence of indexing, space-group determination, profile matching, direct method and Rietveld refinement

for every single powder XRD pattern of a large number of unidentified mixture samples within a limited time frame. A conventional structural analysis should only be performed on the discovered material to identify it in the end. Instead, the structural rank, representing the overall feature of an XRD pattern, was evaluated by referring to structural databases. The structural rank is a rough measure of a structure, but is reasonably defined by a qualitative classification of a large number of measured XRD patterns. The structural rank is described in **Table 2**. The ordering principle (i.e., the philosophy behind the classification) is in the sequence of structural desirability: 1) unidentified structure, 2) existing structure in the crystallography database, but has never been considered as a phosphor, 3) residual starting materials, 4) well-known phosphors, and 5) failure. The most-dramatic rationale for this classification lies in the fact that the residual starting material, which did not participate in the synthesis reaction, was preferred, rather than well-known phosphors, exhibiting promising luminescence. This criterion implies that a composition that results in a certain amount of residual starting materials that remain even after high-temperature firing might potentially lead to the advent of new phases in the next round, but the presence of well-known phosphors, in spite of their high luminescence efficacy, indicates a lower possibility of new phosphors in the next round.

Ranks 1–3 belong to Type IV and ranks 4–7 to Type III. The NSGACMS was designed to minimize the structural rank and maximize the PL intensity simultaneously, so that we could obtain a group of non-dominated phosphor samples, the so-called Pareto front. Because NSGACMS should start with random samples for the first generation, the starting compositions were arbitrarily selected from the SrO-CaO-BaO-La_2O_3-Y_2O_3-Si_3N_4-Eu_2O_3 search space. Several well-known phosphors were detected even in the first generation. If a single objective GA had been used without employing the structural rank, we would have ended up with one of the well-known phosphors. In fact, several well-known, commercially available phosphors, such as $Sr_2Si_5N_8$:Eu^{2+}, $SrSi_2O_2N_2$:Eu^{2+}, Sr_2SiO_4:Eu^{2+}, and $(Sr,Ba)_2SiO_4$:Eu^{2+}, were detected in the first generation (Table S1, Supporting Information). Although the PL intensity of samples containing well-known phosphors was relatively high, their structural ranks were assigned to 11–15, so that the NSGACMS could not primarily select them.

NSGACMS was iterated through 4 consecutive generations. Each generation contained 36 phosphor samples, the PL intensity and structural rank of which were evaluated in a pseudo-HTE manner, classified according to the Pareto optimality theory,[27] and then plotted in **Figure 3**. Because there is no intermediate rank number appearing in Figure 3, one might wonder why we classified the structural ranks so precisely. However, it is just a coincidence that we do not see the intermediate structural ranks in Figure 3. The auxiliary NSGACMS results in the supporting information, which confirm the validity of the proposed strategy, clearly show some intermediate structural-rank numbers (Figure S6, Supporting Information).

A group of points interconnected with a gray straight line is called a Pareto group. No point in a Pareto group dominates the others in the same Pareto group. All of the samples in

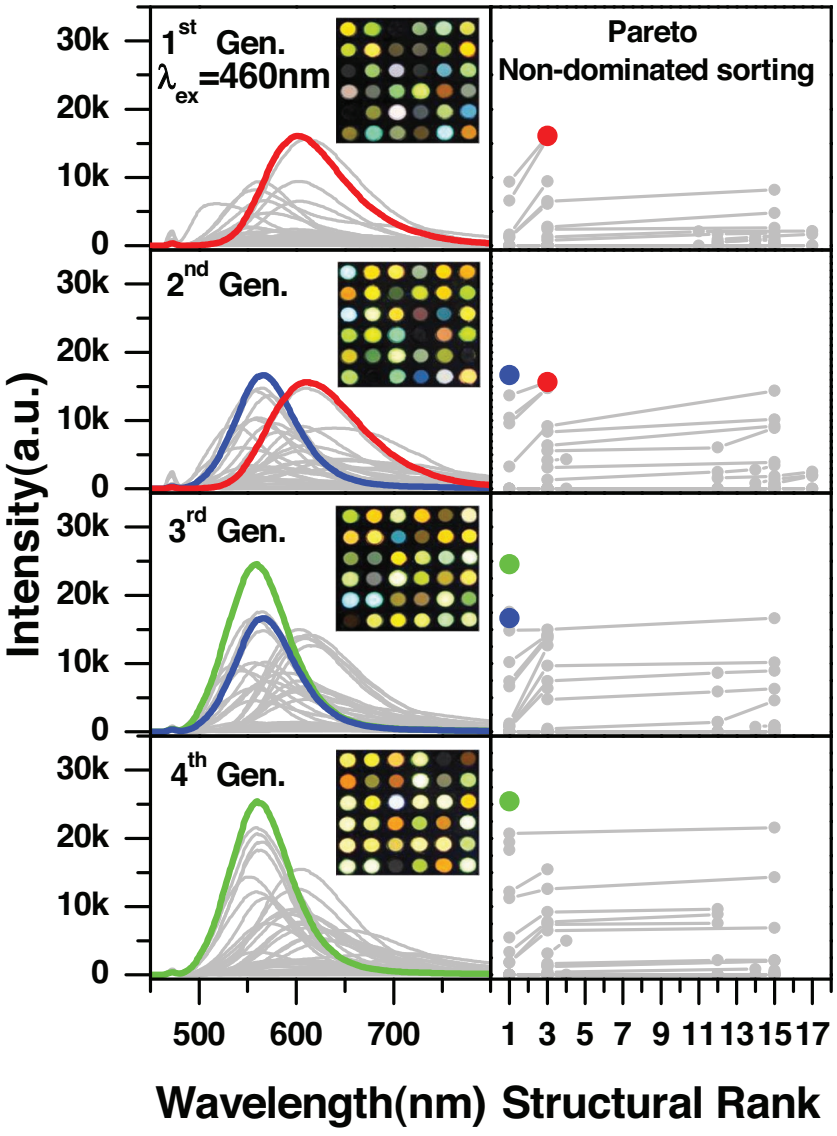

Figure 3. The NSGACMS-execution results: plot of PL intensity versus structural rank for each generation, the so-called Pareto plot, along with emission spectra at 460 nm excitation and actual sample photos taken under a 365 nm UV lamp. The elitist samples are marked in the same color. The green and blue colors represent "Unknown1", which eventually turned out to be $La_{4-x}Ca_xSi_{12}O_{3+x}N_{18-x}$:$Eu^{2+}$ and the red represents "Unknown2", which was indexed as another monoclinic phase. The composition, PL-intensity, structural-rank and phase-identification data are to be found in Table S1, Supporting Information.

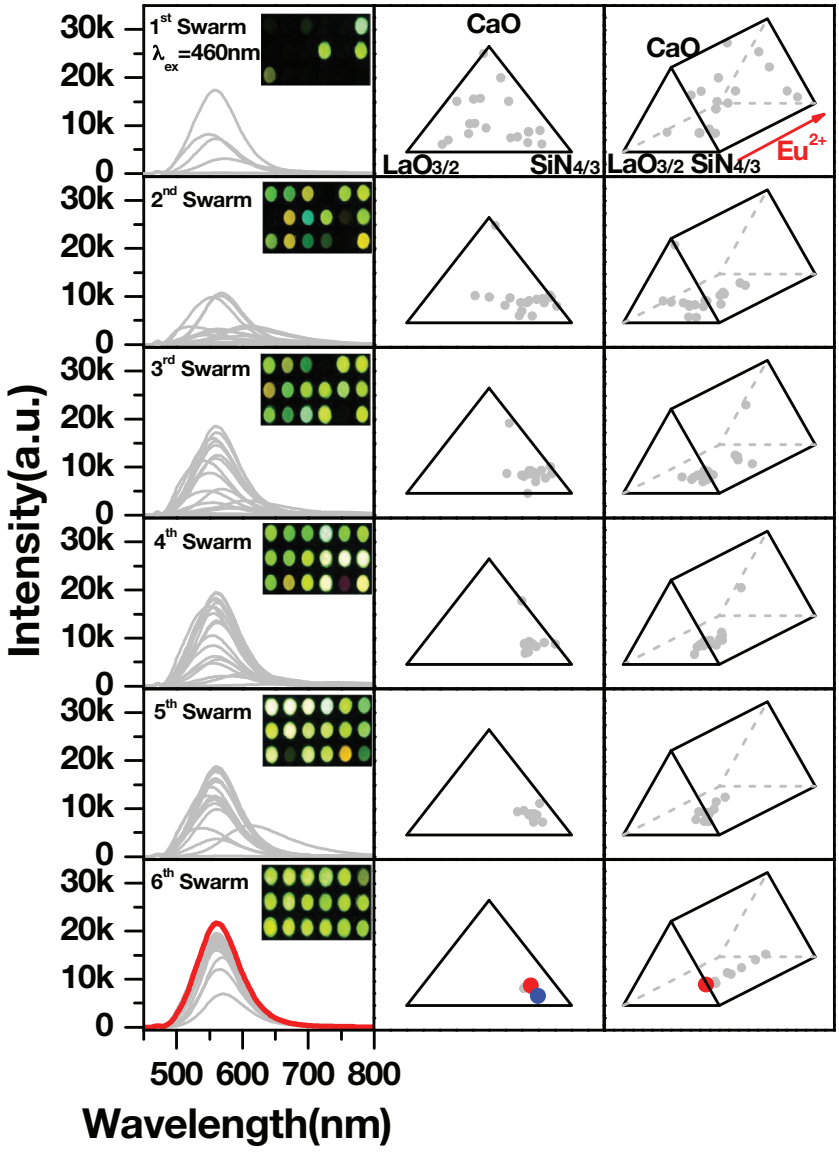

Figure 4. The PSOCMS-execution results: instantaneous swarm positions in CaO-La_2O_3-Si_3N_4-Eu_2O_3 quaternary composition space up to the sixth swarm, showing a rapid convergence to an optimum point. The Eu^{2+} activator concentration ranged from 0 to 10 mol%. The ternary CaO-La_2O_3-Si_3N_4 composition space is also presented for better understanding of the host compositions. The red dot represents the best sample in terms of PL intensity and the blue dot indicates $La_{4-x}Ca_xSi_{12}O_{3+x}N_{18-x}$:$Eu^{2+}$ ($x = 1.456$). Emission spectra at 460 nm excitation and actual sample photographs taken under a 365 nm UV lamp are shown. The composition data, along with the PL intensity, are provided in Table S2, Supporting Information.

each generation were classified into several Pareto groups, and dummy fitness values were assigned to each sample based on a so-called sharing criterion. Because the population size (36) adopted for the NSGACMS was not large enough to produce a typical, densely populated Pareto front, and also because the structural rank was a discrete parameter, the Pareto front in the second, third and fourth generations fortuitously consisted of only 1 sample. The 1-sample Pareto front did not impair the NSGACMS, but rather facilitated the convergence to a new Type-IV phosphor. Both the PL intensity and the structural rank were obviously improved as the NSGACMS went through 4 generations, indicating that a certain degree of evolution took place. A notable Type-IV phosphor with acceptable PL intensity appeared in the second generation and later in the third and fourth generation, as highlighted in blue and green. The composition, PL intensity, structural rank and constituent phases for all of the samples through 4 consecutive generations are listed in Table S1, Supporting Information.

The number of Type-IV samples with the structural rank of 1–3 kept increasing throughout the 4 generations. If we had proceeded to further generations, the number would have increased further and we would have gotten closer to an optimum composition with a higher PL intensity, while the unknown structure was maintained. However, we stopped the NSGACMS at the fourth generation and scrutinized the composition of the promising samples marked in green and blue in Figure 3, which are designated as "Unknown1" in the compound libraries (Table S1, Supporting Information), respectively. The composition of "Unknown1" centered on the CaO-La_2O_3-Si_3N_4-Eu_2O_3 quaternary composition. It was more economical to execute the composition fine-tuning in this reduced composition range, rather than further iterations of the NSGACMS. To achieve efficient screening of this quaternary composition, and to narrow the possibility of discovery, we employed PSOCMS.

PSO, which is comparable to GA in terms of optimization performance, is a population-based heuristic inspired by the social behavior of swarms.[28] Unlike GA, however, PSO has never been coupled with the combi-chem of inorganic functional materials, although it has proven to be versatile for many other optimization tasks. Whereas GA works best in the discrete-decision parameter space, PSO has more effect in the continuous-decision parameter space. In this regard, NSGACMS would work best for preliminary screening in a relatively large search space, while PSOCMS would be more suitable for the ensuing fine-tuning processes in a limited search space, indicating that the combination of NSGA and PSO would be of great help to facilitate the discovery of new Type-III and Type-IV phosphors.

Figure 4 shows 6 consecutive swarms in the triangular-prism-shaped CaO-La_2O_3-Si_3N_4-Eu_2O_3 quaternary composition space. Only the PL intensity at a 460 nm excitation was used as the single objective function in the PSOCMS. The structural information was not taken into account for PSO because most samples did not deviate from the structure of "Unknown1" (Table S1, Supporting Information). The swarm size (18) was reduced to only one-half the population size adopted for the

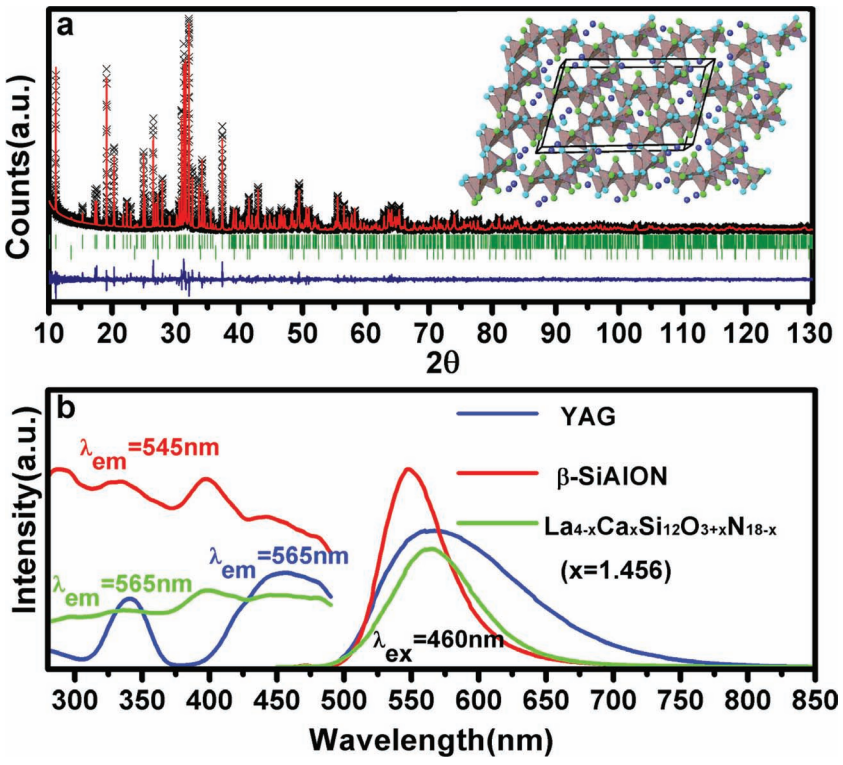

Figure 5. a) The structural determination results for $La_{4-x}Ca_xSi_{12}O_{3+x}N_{18-x}:Eu^{2+}$ (x = 1.456): synchrotron XRD along with the Rietveld refinement fits. Experimental (X) and theoretical (solid line) results, reflectance positions (vertical bars), and the difference between the observed and calculated intensities (solid line) at the bottom (R_p = 8.6377, R_{wp} = 11.1829, R_{exp} = 8.9558, R_I = 5.9797, χ = 1.249) are shown. The inset is the schematic of the refined structure. b) The emission and excitation spectra of $La_{4-x}Ca_xSi_{12}O_{3+x}N_{18-x}:Eu^{2+}$ (x = 1.456) with a Eu^{2+} concentration of 4 mol%, along with the emission spectra of commercially available LED phosphors such as β-SIALON (provided by Samsung LED) and YAG (provided by Nichia). The excitation wavelength for the emission spectrum was 460 nm and the emission probe wavelength for the excitation spectrum is the emission-peak location of each phosphor.

NSGACMS, since the search space was significantly reduced. The sixth swarm was congested in a small composition area and thereby provided a converged final composition with a promising PL intensity, although the structure still remained unknown.

The composition with the highest PL intensity is marked as a red dot in the congested composition area of the sixth swarm (Figure 4). Synchrotron powder XRD (**Figure 5**a), neutron powder diffraction (Figure S3, Supporting Information), selected-area electron diffraction (SAED) (Figure S4, Supporting Information), and the ensuing structural determination process identified the discovered the new Type-IV phosphor, marked as the red dot, to be $La_{4-x}Ca_xSi_{12}O_{3+x}N_{18-x}:Eu^{2+}$ (x = 1.456) with a monoclinic lattice in the $C2$ space group. The detailed structural determination process is described in the supporting information. The stoichiometry of $La_{4-x}Ca_xSi_{12}O_{3+x}N_{18-x}:Eu^{2+}$ (x = 1.456) is marked as the blue dot in Figure 4. This structure was maintained in the x range from 1.2 to 1.6 with acceptable PL intensity, and the emission color changed from green to yellow as x increased. There is a slight difference between the processing composition (red dot) obtained from PSOCMS and the actual stoichiometry (blue dot) identified by the structural analysis. Such a slight difference between the processing composition and the actual stoichiometry is typical in multicompositional solid-state synthesis. The presence of a certain glassy phase including Ca and La in the final sample and impurities in the starting materials are responsible for the discrepancy, which is described in detail in the supporting information. The refined atomic position, thermal factor and occupancy data, along with the lattice parameters for $La_{4-x}Ca_xSi_{12}O_{3+x}N_{18-x}:Eu^{2+}$ (x = 1.456), are summarized in Table S3, Supporting Information.

The emission and excitation spectra show a typical 4f-5d transition of divalent europium activators (Figure 5b), and the spectral distribution and PL intensity of the $La_{4-x}Ca_xSi_{12}O_{3+x}N_{18-x}:Eu^{2+}$ (x = 1.456) is suitable for use in WLEDs. It should be noted that a novel, practical Type-IV phosphor was finally identified, although we started from completely random compositions without considering the materials chemistry. This phosphor could be comparable to well-established, commercially available LED phosphors, if its PL properties were slightly improved by the conventional powder refinement process, which has not yet been done.

In addition to $La_{4-x}Ca_xSi_{12}O_{3+x}N_{18-x}:Eu^{2+}$, two more novel phosphors were also discovered during the NSGACMS. Another new Type-IV phosphor is highlighted in red in Figure 3 and marked as "Unknown2" (Table S1, Supporting Information and Table S4, Supporting Information). The ensuing PSOCMS was again implemented in the reduced search space, SrO-CaO-BaO-Si_3N_4. The detailed composition for "Unknown2" is presented in Table S1, Supporting Information. This new phosphor, designated as "Unknown2", was indexed as a monoclinic phase with possible space groups such $C2$, Cm, or $C2/m$ in the same extinction group ($C1\_1$). Another new Type-III phosphor, which was identified as having the same structure as $Ca_{15}Al_2Si_{18}O_{10}N_{30}$ in a cubic structure with the space group $Pa\bar{3}$,[30] also appeared during the NSGACMS. However, we do not go into the details of these new Type-IV and Type-III phosphors here for the sake of brevity. It should also be noted that we have focused on the discovery of $La_{4-x}Ca_xSi_{12}O_{3+x}N_{18-x}:Eu^{2+}$ because its luminescent properties are superior to any others from a practical point of view. The details surrounding the structural and PL properties of the other new Type-IV and Type-III phosphors will be published separately soon.

To confirm the validity of the proposed method, the NSGACMS was re-executed using a different first generation. Despite the adoption of a completely different first generation, the same new Type-IV phosphor was identified in this confirmative NSGACMS implementation, (Figure S6, Supporting

Information and Table S4, Supporting Information). The ensuing PSOCMS was also reimplemented by adopting a different first swarm. As a result, a similar convergence on $La_{4-x}Ca_xSi_{12}O_{3+x}N_{18-x}:Eu^{2+}$ was obtained (Figure S6, Supporting Information and Table S5, Supporting Information). This proves that the proposed strategy involving NSGACMS, PSOCMS and the structural rank works.

4. Conclusions

In conclusion, we have discovered a novel phosphor for use in WLEDs, $La_{4-x}Ca_xSi_{12}O_{3+x}N_{18-x}:Eu^{2+}$. NSGACMS was implemented for preliminary screening and the ensuing fine-tuning was achieved by PSOCMS. The structural rank, which is indicative of the novelty of a phosphor structure, was introduced as an objective function along with the PL intensity, to avoid converging on well-known, established phosphors. The proposed methodology will appeal not only to phosphor researchers, but also to scientists or engineers engaged in all other advanced-materials research fields. In particular, this strategy will work best for the discovery of inorganic functional materials, (e.g., active materials for Li-battery anodes/cathodes, materials for solid-oxide fuel cells, compound semiconductors, high-T_c superconducting materials, dielectric materials, new metal alloys, structural ceramics, nanomaterials).

5. Experimental Section

The commercially available starting materials in the powdered state, CaO (Kojundo, 99.9%), SrO (Kojundo, 98%), BaO (Kojundo, 99% UP), La_2O_3 (Kojundo, 99.99%), Y_2O_3 (Kojundo, 99.9%), α-Si_3N_4 (Aldrich, unreported), α-Si_3N_4 (Ube, unreported) and Eu_2O_3 (Kojundo, 99.9%), were separately ground manually for several hours to adapt them to the dispensing system. A so-called combi-chem container, a specially designed sample container made of BN (80 × 40 × 20 mm), which involved 18 sample sites that were 8.5 mm in diameter and 16 mm in depth, was devised for the high-throughput dispensing, mixing, grinding and firing of a large number of samples. The total amount of raw materials at each sample site was around 0.3 g, which led to a sufficient amount of final phosphor powder available for use in any of the conventional characterizations. Exact amounts of the raw materials were weighed and dispensed automatically to the sample sites using a powder-extruder system in a high-throughput manner with a robotic platform (Swave, ChemSpeed Tech Co., Ltd.). The mixing and grinding were executed by vibrating the combi-chem containers with pins inserted inside the sample sites. The mixed raw materials in the combi-chem container were fired at 1525 °C for 4 h under a N_2 gas flow (500 ml min^{-1}) in a sealed tube furnace. Two combi-chem containers (i.e., 36 samples) were fired simultaneously. A video showing the entire high-throughput process is available elsewhere.[34]

Each sample synthesized in both the NSGACMS and PSOCMS was ground and subjected to X-ray diffraction (XRD) and photoluminescence (PL) analysis. The emission spectra were monitored at 460 nm excitation, which simulated an InGaN LED light source, with the samples being left in the combi-chem containers in a high-throughput manner using an in-house-fabricated continuous-wave (CW) PL system equipped with a xenon lamp. Finally, the pinpointed sample was examined using synchrotron radiation X-ray diffraction (SR-XRD), neutron diffraction, transmission electron microscopy (TEM), energy-dispersive spectroscopy (EDS), X-ray photoelectron spectroscopy (XPS) and inductively coupled plasma (ICP) mass spectrometry. The SR-XRD measurements of the selected sample were made at the 8C2 high-resolution powder-diffraction beamline at the Pohang Accelerator Laboratory (PAL), and the neutron diffraction was carried out at the high-resolution powder diffraction beamline at the Korea Atomic Energy Research Institute.

Further details of the crystal-structure investigations may be obtained from the Fachinformationszentrum Karlsruhe, 76344 Eggenstein-Leopoldshafen (Germany), on quoting the depository number CSD-424186.

Supporting Information

Supporting Information is available from the Wiley Online Library or from the author.

Acknowledgements

W.B.P. and N.S. contributed equally to this work. This work was supported by the IT R&D program of MKE/IITA (2009-F-020-01), and partly supported by the WCU (World Class University) program through the Korea Science and Engineering Foundation funded by the Ministry of Education, Science and Technology. We would like to thank Prof. H. G. Cho at Sungkyunkwan University in Korea for the SAED measurement and Prof. Armel Le Bail, at the University of Maine in France, for his helpful discussions of the structural determination of our discovered material.

Received: September 6, 2011
Revised: December 15, 2011
Published online: March 7, 2012

[1] E. Danielson, J. H. Golden, E. W. McFarland, C. M. Reaves, W. H. Weinberg, X. D. Wu, *Nat. Mater.* **1997**, *389*, 944.
[2] E. Danielson, M. Devenney, D. M. Giaquinta, J. H. Golden, R. C. Haushalter, E. W. McFarland, D. M. Poojary, C. M. Reaves, W. H. Weinberg, X. D. Wu, *Science* **1998**, *279*, 837.
[3] J. Wang, Y. Yoo, C. Gao, I. Takeuchi, X. Sun, H. Chang, X.-D. Xiang, P. G. Schultz, *Science* **1998**, *279*, 1712.
[4] X.-D. Sun, K.-A. Wang, Y. Yoo, W. G. Wallace-Freedman, C. Gao, X.-D. Xiang, P. G. Schultz, *Adv. Mater.* **1997**, *9*, 1046.
[5] X.-D. Sun, C. Gao, J. Wang, X.-D. Xiang, *Appl. Phys. Lett.* **1997**, *70*, 3353.
[6] T. X. Sun, *Biotechnol. Bioeng.* **1998**, *61*, 193.
[7] K.-S. Sohn, I. W. Zeon, H. Chang, S. K. Lee, H. D. Park, *Chem. Mater.* **2002**, *14*, 2140.
[8] K.-S. Sohn, J. M. Lee, N. Shin, *Adv. Mater.* **2003**, *15*, 2081.
[9] A. K. Sharma, K. H. Son, B. Y. Han, K.-S. Sohn, *Adv. Funct. Mater.* **2010**, *20*, 1750.
[10] A. K. Sharma, C. Kulshreshtha, K.-S. Sohn, *Adv. Funct. Mater.* **2009**, *19*, 1705.
[11] T.-S. Chan, Y.-M. Liu, R.-S. Liu, *J. Comb. Chem.* **2008**, *10*, 847.
[12] L. Chen, Y. Fu, G. Zhang, J. Bao, C. Gao, *J. Comb. Chem.* **2008**, *10*, 401.
[13] L. Chen, J. Bao, C. Gao, *J. Comb. Chem.* **2004**, *6*, 699.
[14] T.-S. Chan, C.-C. Kang, R.-S. Liu, L. Chen, X.-N. Liu, J.-J. Ding, J. Bao, C. J. Gao, *J. Comb. Chem.* **2007**, *9*, 343.
[15] E. F. Schubert, J. K. Kim, *Science* **2005**, *308*, 1274.
[16] N. Hirosaki, R.-J. Xie, K. Kimoto, T. Sekiguchi, Y. Yamamoto, T. Suehiro, M. Mitomo, *Appl. Phys. Lett.* **2005**, *86*, 211905.
[17] K. Uheda, N. Hirosaki, Y. Yamamoto, A. Naito, T. Nakajima, H. Yamamoto, *Electrochem. Solid State Lett.* **2006**, *9*, H22.
[18] a) R.-J. Xie, N. Hirosaki, T. Suehiro, F.-F. Xu, M. Mitomo, *Chem. Mater.* **2006**, *18*, 5578; b) Y. Q. Li, A. C. A. Delsing, G. de With, H. T. Hintzen, *Chem. Mater.* **2005**, *17*, 3242.

[19] Y. Q. Li, A. C. A. Delsing, G. de With, H. T. Hintzen, *Chem. Mater.* **2005**, *17*, 3242.
[20] E. J. Amis, *Nat. Mater.* **2004**, *3*, 83.
[21] I. Takeuchi, O. O. Famodu, J. C. Read, M. A. Aronova, K.-S. Chang, C. Craciunescu, S. E. Lofland, M. Wuttig, F. C. Wellstood, L. Knauss, A. Orozco, *Nat. Mater.* **2003**, *2*, 180.
[22] J. Greeley, T. F. Jaramillo, J. Bonde, I. Chorkendorff, J. K. Kørskov, *Nat. Mater.* **2006**, *5*, 909.
[23] H. Koinuma, I. Takeuchi, *Nat. Mater.* **2004**, *3*, 429.
[24] W. F. Maier, K. Stöwe, S. Sieg, *Angew. Chem. Int. Ed.* **2007**, *46*, 6016.
[25] R. Potyrailo, K. Rajan, K. Stoeww, I. Takeuchi, B. Chisholm, H. Lam, *ACS Comb. Sci.* **2011**, *13*, 579.
[26] J. H. Holland, *Adaptation in natural and artificial systems*, The University of Michigan, Ann Arbor, MI **1975**.
[27] N. Srinivas, K. Deb, *Evolutionary Comput.* **1994**, *2*, 221.
[28] J. Kennedy, R. Eberhart, *Proc. IEEE Int. Conf. Neural Networks* **1995**, *4*, 1942.
[29] M. Bulut, L. E. M. Gevers, J. S. Paul, I. F. J. Vankelecom, P. A. Jacobs, *J. Comb. Chem.* **2006**, *8*, 168.
[30] F. Ottinger, Ph.D. Thesis, Eidgenössischen Technischen Hochschule, Zürich, Diss. ETH Nr. **2004**, 15624.
[31] C. Klanner, D. Farrusseng, L. Baumes, M. Lengliz, C. Mirodatos, F. Schüth, *Angew. Chem. Int. Ed.* **2004**, *43*, 5347.
[32] O. C. Gobin, F. Schüth, *J. Comb. Chem.* **2008**, *10*, 835.
[33] D. Wolf, O. V. Buyevskaya, M. Baerns, *Appl. Catal. A.* **2000**, *200*, 63.
[34] W. B. Park, S. P. Singh, M. Pyo, K.-S. Sohn, *J. Mater. Chem.* **2011**, *21*, 5780.